

Ambivalent Behavior of Ytterbium in the Pseudobinary System YbMo_6S_8 - YbMo_6Se_8

JEAN-MARIE TARASCON, DAVID C. JOHNSON, and M. J. SIENKO*

Received August 20, 1981

The pseudobinary system YbMo_6S_8 - YbMo_6Se_8 has been investigated for its magnetic and superconducting behavior in an attempt to find out why, of the rare earth molybdenum chalcogenides, ytterbium is anomalously high in the sulfide series and anomalously low in the selenide series for onset of superconductivity. Mixed-solid solutions have been prepared from ultrapure starting elements and characterized by X-ray, static Faraday susceptibility, and ac superconductivity studies. The superconductivity of end member YbMo_6S_8 has been confirmed, but that of YbMo_6Se_8 has not. The superconducting critical temperature shows a monotonic decrease from 8.65 K for the fully sulfided member to <1.6 K for all selenium. Faraday susceptibility studies over the range 1.6-300 K show Curie-Weiss behavior corresponding to 3.3% Yb^{3+} ($4f^{13}$) in YbMo_6S_8 and 1.3% in YbMo_6Se_8 . Thus, the nonappearance of superconductivity in the selenide cannot be attributed to increasing content of pair-breaking paramagnetic ion. Extreme thermal treatment of YbMo_6S_8 up to 1550 °C increased the Yb^{3+} content from 3.3% to 5.2% but depressed T_c only from 8.65 to 7.75 K; similar treatment of YbMo_6Se_8 to 1550 °C increased the Yb^{3+} content from 1.3% to 9.3% but did not result in superconductivity. Superconductivity of the selenide as reported in the literature over the range 4.7-5.8 K could be reproduced with nonstoichiometric material $\text{Yb}_{1\pm x}\text{Mo}_6\text{Se}_8$ ($T_c = 5.6$ -5.8 K), but X-ray studies showed the presence of a second phase corresponding to Mo_6Se_8 , which normally has its own T_c of about 6 K.

Introduction

The ternary molybdenum chalcogenides, MMo_6X_8 , so-called Chevrel phases,¹ have proved to be fascinating puzzles for the problem of correlating physical properties with structural parameters.² When M is a large atom such as lanthanum or lead, there appears to be a unique site on the $\bar{3}$ axis for full unit cell occupancy; when M is a small atom such as copper, there are up to 4 copper atoms per unit cell distributed over 12 sites off the $\bar{3}$ axis. Charge transfer from M to Mo_6X_8 clusters limits the occupancy to four as it takes but four electrons to fill the single-bonded structure of the Mo_6X_8 cluster network. Many of the ternary molybdenum chalcogenides are superconductors,³ even when M is a magnetic ion.⁴ The superconductivity is generally attributed to the molybdenum d-orbital manifold, and this is disturbed only when magnetic ions sit close to the molybdenum network, as when the magnetic ions are small and occupy the multiple sites.

The structure of the ternary molybdenum chalcogenides is shown in Figure 1. The characteristic structural feature is an Mo_6X_8 cluster with X atoms approximating a cube and Mo atoms being slightly above the centers of the cube faces. Each cube is rotated approximately 25° about its body diagonal ($\bar{3}$ axis) so that the X of one cluster approaches and is bonded to a Mo of a neighboring cluster. The ternary M atoms, when large, sit on the $\bar{3}$ axis between the rotated cubic clusters and, when small, in a double belt of 12 tetrahedral sites disposed around the $\bar{3}$ axis.

In the rare earth sequences (RE) Mo_6S_8 and (RE) Mo_6Se_8 , the critical temperature for onset of superconductivity shows a pronounced falloff from a maximum value at La (6.95 K for LaMo_6S_8 and 11.3 K for LaMo_6Se_8) to a leveling off at approximately 2 K in the sulfide series⁴ and 6 K in the selenide series.⁵ As shown in Figure 2, the ytterbium member is anomalously high in the sulfide series and anomalously low in the selenide series. Neither the cerium nor the europium

members are superconducting at normal pressures above 1.1 K.

Andersen, Klose, and Nohl⁶ have calculated the band structure of PbMo_6S_8 using an atomic sphere, muffin-tin approximation. They find at the Fermi level two partially filled bands—a broad A_{1g} band composed mainly of Mo d_{z^2} orbitals and a much narrower E_g band composed of d_{xy} and $d_{x^2-y^2}$ orbitals. There are two van Hove singularities in the E_g band, and the Fermi level lies close to one of them, but the band calculation cannot decide between them because of uncertainty in the relative position of the A_{1g} band. Magnetic susceptibility studies⁷ on the pseudobinary system PbMo_6S_8 - PbMo_6Se_8 showed an unusual temperature-dependent type of Pauli susceptibility, which confirmed the van Hove singularity. On the basis of comparison of the various superconducting critical temperatures, the present best guess for the relative filling of the E_g band is as shown in Figure 3.

In the BCS theory⁸ the superconducting critical temperature is given by

$$T_c \approx \langle \omega \rangle \exp(-1/NV)$$

where $\langle \omega \rangle$, the mean phonon frequency, measures the stiffness of the lattice, N measures the density of states at the Fermi level (equivalent to the number of canonical forms of equal energy in resonance), and V measures the electron-phonon coupling constant (which can be thought of as the analogue in Jahn-Teller distortion of the coupling constant between orbital motion and the normal modes). In a homologous series such as MMo_6X_8 , where $\langle \omega \rangle$ and V can be crudely approximated as constant, the T_c depends on the density of states N , which in turn depends on the degree of band filling. Generally, T_c increases as N increases. From Figure 3 it can be seen that, in going from PbMo_6S_8 ($T_c = 13.29$ K) to PbMo_6Se_8 ($T_c = 3.89$ K), the degree of band filling is increased but in such a way as to lead to a lower value of N . We rationalize this chemically by noting that selenium has a lower electronegativity than does sulfur; hence, selenium acts as a better donor of electrons to the conduction band than does sulfur. With this line of reasoning, for any divalent $\text{M}^{II}\text{Mo}_6\text{X}_8$ one would

(1) Chevrel, M.; Sergent, M.; Prigent, J. *J. Solid State Chem.* **1971**, *3*, 515.
(2) For an excellent review of structural properties see: Yvon, K. *Curr. Top. Mater. Sci.* **1979**, *3*. For physical properties, see: Fischer, Ø. *Appl. Phys.* **1978**, *16*, 1.

(3) Matthias, B. T.; Marezio, M.; Corenzwit, E.; Cooper, A. S.; Barz, H. E. *Science (Washington, D.C.)* **1972**, *175*, 1465.

(4) Fischer, Ø.; Treyvaud, A.; Chevrel, R.; Sergent, M. *Solid State Commun.* **1975**, *17*, 721.

(5) Shelton, R. N.; McCallum, R. W.; Adrian, H. *Phys. Lett. A* **1976**, *56A*, 213.

(6) Andersen, O. K.; Klose, W.; Nohl, H. *Phys. Rev. B: Solid State* **1978**, *17*, 1209.

(7) Delk, F. S., II; Sienko, M. J. *Inorg. Chem.* **1980**, *19*, 1352.

(8) Bardeen, J.; Cooper, L. N.; Schrieffer, J. R. *Phys. Rev.* **1957**, *106*, 162; **1957**, *108*, 1175.

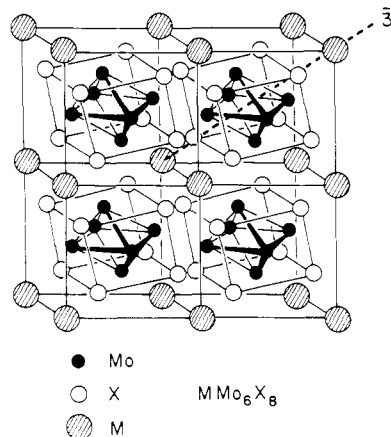


Figure 1. Idealized structure of MMo_6X_8 .

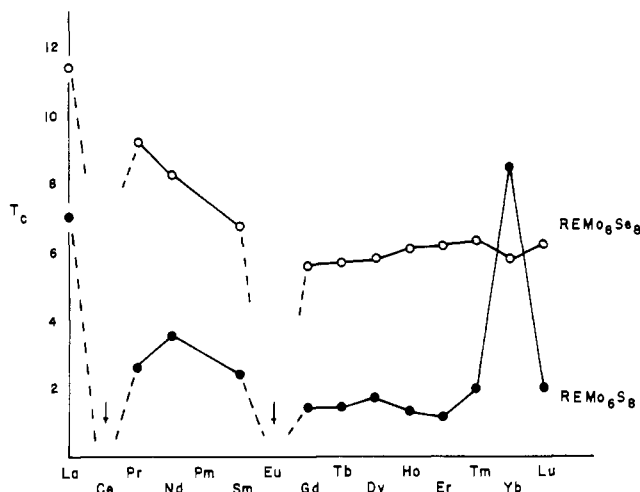


Figure 2. Superconducting critical temperatures T_c vs. rare earth element for the series $(RE)Mo_6S_8$ (filled circles) and $(RE)Mo_6Se_8$ (open circles).

expect that replacing S by Se for X would depress the superconducting critical temperature. Also, as is shown in Figure 3, when we go from a divalent donor situation, $M^{II}Mo_6S_8$, to a trivalent one, $M^{III}Mo_6S_8$, we again get more band filling with a reduction in the density of states. For this reason the T_c of $LaMo_6S_8$ (6.95 K) is lower than that of $PbMo_6S_8$ (13.29 K). What happens now if we replace S by Se in $LaMo_6S_8$? As can be seen from Figure 3, we pass the minimum in the density of states and the better donor character of Se over S fills more of the band and goes to a *higher* density of states, ergo, higher T_c .

The anomaly of Yb in $(RE)Mo_6S_8$ series (Figure 2) is now clear. Yb is generally divalent, in contrast to the other rare earth elements, which are generally trivalent. Yb in $Yb^{II}Mo_6S_8$ fills the E_g band to a lower level (more like $PbMo_6S_8$) than do the other rare earth elements. At this lower level, the density of states is greater and so is T_c . What about $YbMo_6Se_8$? This is an enigma. If it is truly $Yb^{II}Mo_6Se_8$, then compared to that of $(RE)^{III}Mo_6Se_8$, the T_c of $YbMo_6Se_8$ should also be out of line on the high side. In fact, it is lower. Because of the inconsistency in the observed result, we decided it would be interesting to prepare the full series $YbMo_6S_{8-x}Se_x$ and observe what happens stepwise to the superconducting properties. We also wished to measure the low-temperature magnetic susceptibility because of the suspicion that the yttrium in these ternary molybdenum chalcogenides might not be all divalent but partially trivalent. Since Yb^{2+} ($4f^{14}$) is diamagnetic whereas Yb^{3+} ($4f^{13}$, $^2F_{7/2}$, $\mu = 4.54 \mu_B$) is highly paramagnetic, this might provide a convenient means for

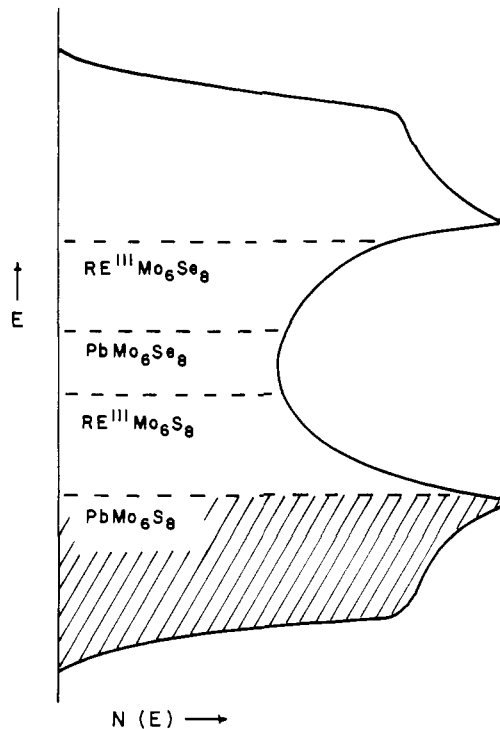


Figure 3. Proposed level of filling of the E_g band for various ternary molybdenum chalcogenides. (The representation here is meant to be only schematic. From M^{II} to M^{III} a rigid-band model is probably acceptable, but replacement of S by Se almost certainly decreases the overall width of the E_g band and probably shifts its position with respect to other bands near the Fermi level. Distortions of the Mo_6 octahedron have been ignored.)

quenching the superconductivity.

In the following, we describe the preparation of the members of the series $YbMo_6S_{8-x}Se_x$ ($x = 0-8$), the measurement of their superconducting critical temperatures, and the measurement as a function of temperature of the magnetic susceptibilities. In the course of the investigation, we also studied the effect of going off stoichiometry, both in the chalcogen content and in that of the ternary element.

Experimental Section

Sample Preparation. The compounds described here were prepared from ultrapure elements: Yb (99.99% from United Mineral and Chemical Corp.), Mo (99.95% from United Mineral and Chemical Corp.), S and Se (99.9999% from Atomergic Chemetals Corp.). The Mo powder was reduced prior to use at 1000 °C under a flow of hydrogen and stored in a vacuum desiccator until needed.

Appropriate amounts of the elements to form 1-g samples of the mixed compounds $YbMo_6S_{8-x}Se_x$ ($x = 0-8$ in unit steps) were placed in previously degassed silica tubes, degassed again at 10^{-6} torr, and sealed. All the tubes were placed together in a box furnace, the temperature of which was uniformly and slowly raised to 1050 °C over the course of 5 days. After 24 h at 1050 °C, the samples were cooled in air and vigorously shaken so as to homogenize. They were immediately reheated to 1100 °C, kept there for 48 h, and then air-cooled. The samples were removed to a helium Dri-Lab where they were opened and thoroughly ground. After they were resealed in new degassed silica ampules, which were sealed in bigger ones, the samples were heated as previously described. The samples were then heated at 1220 °C for 96 h and finally cooled in air. The resulting materials were fine, homogeneous, gray-black powders.

Powder X-ray Diffraction. X-ray diffraction photographs were made by using a 114.6-mm diameter Debye-Scherrer camera with nickel-filtered $Cu K\alpha$ radiation. Lines were indexed with the aid of a Fortran program that calculated the positions and intensities of possible reflections from available single-crystal data. A least-squares fit, with correction for absorption and camera radius error, was performed by using all lines with $\theta(hkl) > 30^\circ$ that could be indexed unambiguously. The procedure yields lattice parameters with errors

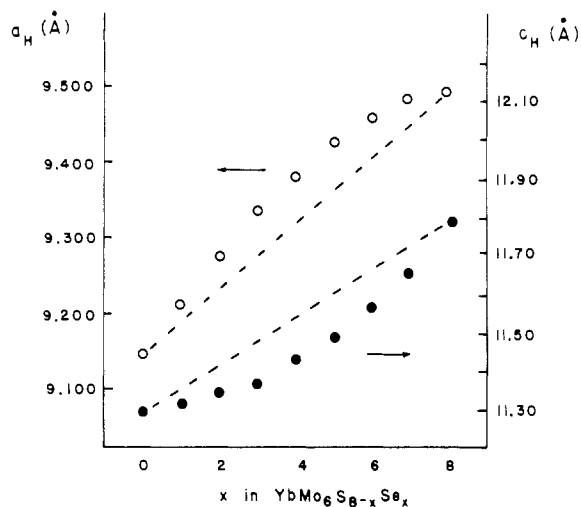


Figure 4. Hexagonal unit cell parameters as a function of selenium replacement for sulfur in $\text{YbMo}_6\text{S}_{8-x}\text{Se}_x$.

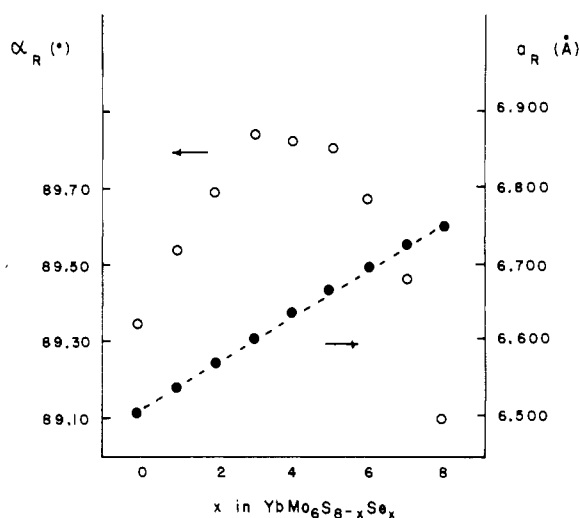


Figure 5. Rhombohedral unit cell parameters as a function of selenium replacement for sulfur in $\text{YbMo}_6\text{S}_{8-x}\text{Se}_x$.

of less than one part per thousand. All samples were single phase to X-ray analysis except as noted below.

Superconducting Transition Determination. The transition to the superconducting state was monitored by using an ac mutual-inductance apparatus, which has been described elsewhere.⁹ In this device, the detection system is a primary coil with two opposed external secondary coils wound symmetrically about it. The sample was placed in one of the secondary coils, and onset of superconductivity is signaled by an abrupt increase in magnetic shielding when the sample becomes perfectly diamagnetic. Temperature was measured by using a calibrated CryoCal germanium thermometer, which was checked against the boiling point of helium and the transition temperature of lead and niobium. The T_c value was taken as the temperature at which the inductively measured transition was half complete. The width of the transition is the temperature difference between the points where the transition is 10% and 90% complete.

Magnetic Susceptibility Measurement. Magnetic susceptibilities were measured from T_c to room temperature by the Faraday technique with use of the apparatus previously described.¹⁰ The temperature was measured with a germanium resistance thermometer (from CryoCal) in the range 1.5–100 K and with a copper/constantan thermocouple in the range 100–300 K. Forces were measured with a Cahn RG electrobalance. The field gradient was calibrated by using $\text{HgCo}(\text{SCN})_4$ as a standard. Samples were held in a Spectrosil quartz

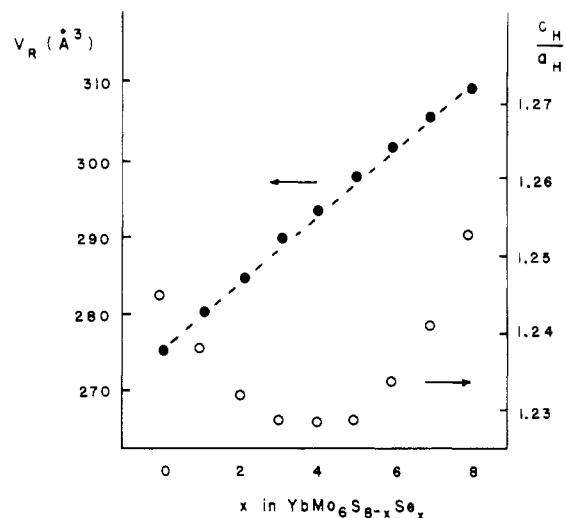


Figure 6. Rhombohedral unit cell volume V_R and hexagonal c/a ratio as a function of x in $\text{YbMo}_6\text{S}_{8-x}\text{Se}_x$.

Table I. Superconducting Critical Temperatures, T_c , for Members of the Series $\text{YbMo}_6\text{S}_{8-x}\text{Se}_x$

x	T_c , K	ΔT_c , K	x	T_c , K	ΔT_c , K
0	8.65 (8.45) ^a	2.9	5	3.26	1.07
1	5.85	1.77	6	2.89	0.86
2	4.23	1.62	7	2.15	0.70
3	3.94	1.1	8	<1.6 (4.7–5.8) ^a	
4	3.48	0.9			

^a T_c values as reported in the literature.^{4,5}

bucket. The reported susceptibilities were field independent and have been corrected for the susceptibility of the bucket.

Results and Discussion

These materials can be indexed completely on the basis of either a hexagonal cell or a rhombohedral cell. Figure 4 gives the hexagonal unit cell parameters a and c as a function of the number of sulfur atoms replaced by selenium. Both a and c are seen to deviate from the linearity expected for Vegard's law. Figure 5 shows the course of the rhombohedral parameters a_R and α_R . Although a_R is almost precisely linear with x in $\text{YbMo}_6\text{S}_{8-x}\text{Se}_x$, α_R shows a pronounced maximum when half of the sulfur atoms have been replaced by selenium. As indicated previously,⁷ the selenium seems to prefer to avoid the special positions on the $\bar{3}$ axis. The accumulation of Se in the general positions (off the $\bar{3}$ axis) makes α_R approach 90° , lessening the distortion away from a perfectly cubic unit cell. However, the last Se to go in must go on the $\bar{3}$ axis, apparently again restoring the slight elongation of the cube along the body diagonal. Enhanced covalent bonding from S to Se of the chalcogen to the ternary element along $\bar{3}$ would be consistent with this distortion.

Figure 6 shows what happens to the hexagonal c/a ratio and the rhombohedral unit cell volume as Se replaces S in YbMo_6S_8 . In some cases, it has been possible to correlate an increase of superconducting critical temperature with a decrease of rhombohedral angle¹¹ or an increase of unit cell volume.¹² However, the broadest correlation seems to be with increasing c/a ratio.¹³ On this last basis, from Figure 6 we would expect for the series $\text{YbMo}_6\text{S}_{8-x}\text{Se}_x$ a minimum in the superconducting critical temperature at $x = 4$. Instead, as can be seen from Table I, T_c continues to drop for $x > 4$ and

(9) Fisher, W. G. Ph.D. Thesis, Cornell University, 1978.

(10) Young, J. E., Jr. Ph.D. Thesis, Cornell University, 1971. Schneemeyer, L. F. Ph.D. Thesis, Cornell University, 1978.

(11) Chevrel, R.; Sergent, M.; Fischer, O. *Mater. Res. Bull.* **1975**, *10*, 1169.

(12) Sergent, M.; Chevrel, R.; Rossel, C.; Fischer, O. *J. Less-Common Met.* **1978**, *58*, 179.

(13) Delk, F. S., II; Sienko, M. J. *Solid State Commun.* **1979**, *31*, 699.

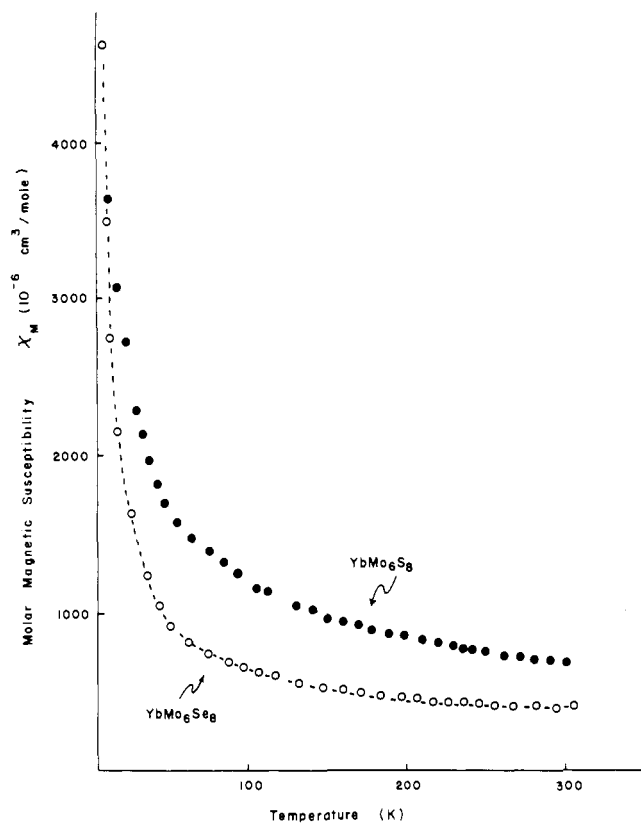


Figure 7. Observed molar magnetic susceptibility of YbMo_6S_8 and of YbMo_6Se_8 as a function of temperature.

indeed reaches its lowest value for $x = 8$. Unexpected, also, is the discrepancy with the literature found for $x = 8$. Whereas we did not find YbMo_6Se_8 to superconduct at all, others have found it to have quite a respectable T_c .

The most common reason for a depressed T_c is the presence of magnetic impurities, as these may produce local fields that can break up the coupling between superconducting electron pairs. Figure 7 shows the observed molar magnetic susceptibilities of the two end members YbMo_6S_8 and YbMo_6Se_8 as a function of temperature. As can be seen, the susceptibility of YbMo_6Se_8 is lower than that of YbMo_6S_8 at all temperatures, implying that YbMo_6Se_8 has fewer magnetic ions and, if anything, should have the higher T_c .

In view of the high purity of the materials and the extreme care taken in their synthesis and characterization, an important question is the source of the paramagnetism in these materials. Yb^{2+} ($4f^{14}$, S_0) is diamagnetic, and there should be only limited Pauli paramagnetism from the conduction electrons. Plots of the raw data, as reciprocal susceptibility vs. temperature (Figure 8), disclosed that the Curie-Weiss law was not obeyed. This is not surprising as the most probable paramagnetic source would be Yb^{3+} ($4f^{13}$, $^2F_{7/2}$).¹⁴ The excited level $^2F_{5/2}$ can be safely ignored, as it is about 10000 cm^{-1} above the ground term $^2F_{7/2}$, but the ground term is split in a cubic crystal field into a lowest Γ_7 level, a Γ_6 that is 68 cm^{-1} higher, and a Γ_3 that is 90 cm^{-1} above Γ_7 . As a result, some temperature dependence of the effective magnetic moment of Yb^{3+} would be expected at low temperatures (below 130 K).

In an attempt to estimate how much Yb^{3+} was actually present in these materials, two procedures were invoked. (a) In one, the observed molar susceptibility of $\text{YbMo}_6\text{S}_{8-x}\text{Se}_x$ at room temperature was corrected for background susceptibility (core diamagnetism, Pauli electron gas) by subtracting the observed molar susceptibility of $\text{PbMo}_6\text{S}_{8-x}\text{Se}_x$ at a corre-

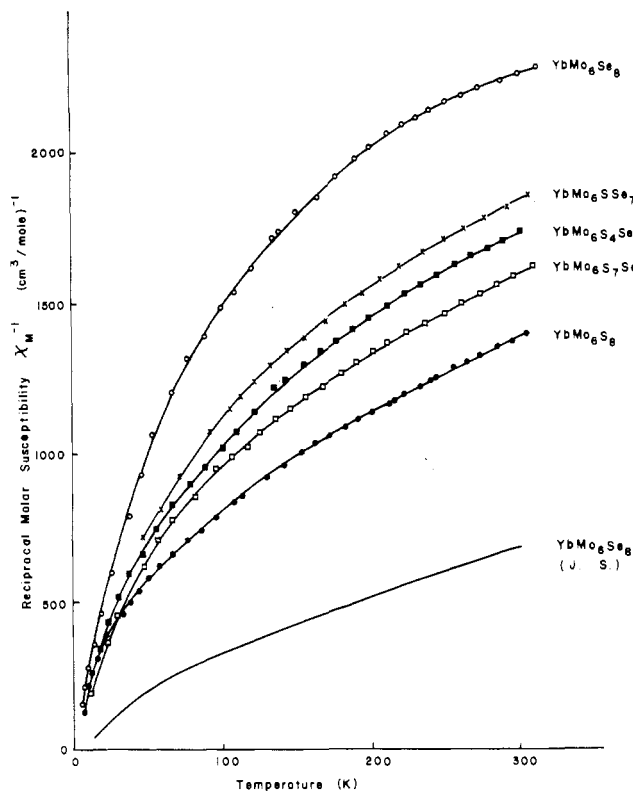


Figure 8. Reciprocal molar magnetic susceptibility vs. temperature for various samples of $\text{YbMo}_6\text{S}_{8-x}\text{Se}_x$. The five uppermost curves correspond to 1220 °C preparations. The bottom curve shows data of Johnson and Shelton.¹⁴

Table II. Room-Temperature Susceptibilities of $\text{MMo}_6\text{S}_{8-x}\text{Se}_x$

x	$10^{-6} \chi_M$		$10^{-6} \times \Delta\chi_M$	μ_{eff}^a μ_B	% Yb^{3+} b
	M = Yb	M = Pb			
0	721	502	219	0.72	2.5
1	615	455	160	0.62	1.9
2	596	427	169	0.64	2.0
3	590	404	186	0.67	2.2
4	577	388	189	0.67	2.2
5	570	384	186	0.67	2.2
6	577	380	197	0.69	2.3
7	535	370	165	0.63	1.9
8	435	352	83	0.45	1.0

^a $\mu_{\text{eff}} = 2.828(\Delta\chi_M T)^{1/2}$. ^b % $\text{Yb}^{3+} = (\mu_{\text{eff}}(\text{obsd})/\mu_{\text{eff}}(\text{for } \text{Yb}^{3+}))^2$.

sponding value of x . The results are shown in Table II. Under the assumption that the difference can be attributed to a localized magnetic moment obeying the Curie law, $\chi = C/T$, with $C = N\mu^2/3k$, we calculate an effective magnetic moment from the relation $\mu_{\text{eff}} = 2.828[(\Delta\chi_M T)]^{1/2}$. Assuming further that the effective moment is generated by a mixture of Yb^{2+} ($\mu = 0$) and Yb^{3+} ($\mu = 4.54 \mu_B$), we can calculate the apparent fraction of Yb^{3+} . As seen from the table, it varies from a high of 2.5% Yb^{3+} in YbMo_6S_8 to a low of 1.0% Yb^{3+} in YbMo_6Se_8 . Not only does the paramagnetic content go in the wrong direction to account for the decreased superconductivity, but also, as noted below, presence of considerable content of Yb^{3+} by itself is not sufficient to quench the superconductivity.

The second method for extracting information about the Yb^{3+} content was to use only the temperature-dependent part of the susceptibility. For this purpose, the observed susceptibility at 300 K was taken to represent the sum of the core diamagnetism, the Pauli susceptibility, and the Van Vleck TIP. χ_{300} was then subtracted from each observed χ_T (at any

(14) Johnston, D. C.; Shelton, R. N. *J. Low Temp. Phys.* 1977, 26, 561.

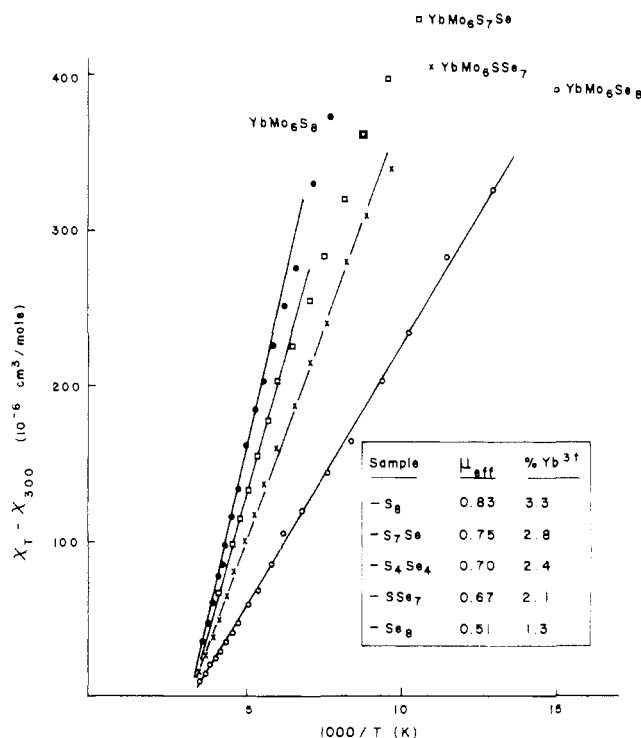


Figure 9. Observed molar susceptibility less the room-temperature value vs. reciprocal temperature for various samples of $\text{YbMo}_6\text{S}_{8-x}\text{Se}_x$. The slope of the line in the high-temperature region gives directly the Curie constant for the localized moment. Departures from linearity in the low-temperature region would be expected because of crystal-field effects on the moment of Yb^{3+} .

Table III. Crystallographic Data and Superconducting Critical Temperatures for Nonstoichiometric YbMo_6Se_8

nominal compn	a , Å	c , Å	c/a	T_c , K	other phases
$\text{YbMo}_6\text{Se}_{8.3}$	9.483	11.888	1.2536	<1.6	MoSe_2
YbMo_6Se_8	9.485	11.890	1.2535	<1.6	none
$\text{YbMo}_6\text{Se}_{7.7}$	9.487	11.894	1.2537	<1.6	none
$\text{YbMo}_6\text{Se}_{7.5}$	9.486	11.895	1.2539	<1.6	none
YbMo_6Se_7	9.487	11.897	1.2541	<1.6	Mo (?)
$\text{YbMo}_6\text{Se}_{6.5}$	9.487	11.897	1.2540	<1.6	Mo
YbMo_6Se_6	9.487	11.896	1.2539	<1.6	$\text{Mo} + ?$
$\text{Yb}_{1.2}\text{Mo}_6\text{Se}_8$	9.485	11.892	1.2538	5.65 ($\Delta T_c = 1.2$)	Mo_6Se_8

temperature) and the difference plotted as a function of reciprocal temperature. The results are shown in Figure 9. The slope of each line gives the Curie constant directly, and $\mu_{\text{eff}} = 2.828C^{1/2}$. As can be seen, the results for percent Yb^{3+} are consistent, showing a high of 3.3% in YbMo_6S_8 and a low of 1.3% in YbMo_6Se_8 .

Because our observed value of T_c for YbMo_6Se_8 was so much lower than that reported in the literature, we essayed to manipulate the deviation from stoichiometry in order to maximize the T_c . For the tin molybdenum sulfide, Delk and Sienko¹⁵ had found that removal of some of the sulfur, presumably from the special sites on the $\bar{3}$ axis, raised T_c from 11.25 K for SnMo_6S_8 to 13.56 K for $\text{SnMo}_6\text{S}_{7.5}$. Table III shows the results of trying to go off stoichiometry for $\text{YbMo}_6\text{Se}_{8-x}$. None of the compounds is superconducting. Furthermore, as the selenium content goes from 8.3 to 6, impurity phases appear in the X-ray diffraction photographs— MoSe_2 when the selenium content is greater than 8 and Mo when the selenium content is less than 7.5. The homogeneity range of the Chevrel phase appears to be Yb

Table IV. Crystallographic Data and Superconducting Critical Temperatures for Nonstoichiometric YbMo_6S_8

nominal compn	a , Å	c , Å	c/a	T_c , K	ΔT_c , K	other phases
$\text{YbMo}_6\text{S}_{8.3}$	9.152	11.394	1.2450	8.15	3.3	MoS_2
YbMo_6S_8	9.150	11.392	1.2450	8.65	2.9	none
$\text{YbMo}_6\text{S}_{7.7}$	9.156	11.408	1.2460	8.75	2.1	none
$\text{Yb}_{1.2}\text{Mo}_6\text{S}_8$	9.148	11.349	1.2406	8.35	3	none
YbMo_6S_8 (1520 °C)	9.161	11.384	1.2427	7.75	2.1	none

$\text{Mo}_6\text{Se}_{8-7.5}$, in which range the hexagonal a parameter stays constant and c increases slightly. This would be consistent with the expectation that there is no change in the general position occupancy but that the deficit selenium comes out of the special positions (on the $\bar{3}$ axis).

The most surprising result is shown by the last entry in Table III. When the nonstoichiometry was pushed in the direction of having ytterbium in excess, the resulting sample was observed to be superconducting with a T_c of 5.65 K! This value, however, is almost the same as that reported for Mo_6Se_8 ($T_c = 6.3$ K).¹⁶ Indeed, examination of the X-ray diffraction pattern clearly showed the lines of Mo_6Se_8 . As a result, we believe that the literature-reported superconductivity for YbMo_6Se_8 was actually due to the presence of Mo_6Se_8 in the specimens. This would not be surprising, as the Chevrel phases are notoriously difficult to prepare in a pure condition.

In order to calibrate our findings on the ytterbium–molybdenum–selenium system, we repeated the nonstoichiometry experiments with ytterbium–molybdenum–sulfur. The results are shown in Table IV. Any sulfur content above 8 immediately showed up as a second phase, MoS_2 . Dropping the sulfur content below 8 produced little or no change in T_c . Having excess ytterbium also seemed to have little effect on the superconductivity. The biggest effect, and that was a depression of only 1 K in T_c , was obtained by a drastic increase in the annealing temperature from 1220 to 1520 °C. The last sample shown in Table IV was electronically welded in a molybdenum capsule and kept at 1520 °C for 5 h. X-ray diffraction showed no impurity phase, but there was a slight change in lattice parameters (a goes from 9.15 to 9.161 Å; c goes from 11.384 to 11.392 Å) as well as the T_c depression from 8.65 to 7.75 K. Magnetic susceptibility measurements on this sample (Figure 10) showed a definite increase in paramagnetism corresponding to an increase of Yb^{3+} content from 3.3% to 5.2%. Noteworthy is the fact that a decided increase in Yb^{3+} content is only mildly effective in reducing T_c .

Similar results were obtained on a YbMo_6Se_8 sample heated at 1550 °C for 16 h. The a lattice parameter showed a small increase (from 9.485 to 9.496 Å) whereas the c parameter stayed constant (at 11.890 Å). Furthermore, the Yb^{3+} content increased from 1.3% to 9.3% (Figure 10). Still, however, there was no superconductivity above 1.5 K.

Qualitatively, the above findings are consistent with the density-of-states diagram presented in Figure 3. Our magnetic results clearly show that ytterbium is mainly divalent in the Chevrel phases compared to the other rare earth elements, which are trivalent. Fewer electrons are donated to the E_g band, and the level filling is lower than shown in Figure 3 for $(\text{RE})^{III}\text{Mo}_6\text{S}_8$ and $(\text{RE})^{III}\text{Mo}_6\text{Se}_8$. As can be seen, this means increased $N(E)$ (ergo, T_c) for $\text{Yb}^{II}\text{Mo}_6\text{S}_8$ and decreased $N(E)$ for $\text{Yb}^{III}\text{Mo}_6\text{Se}_8$. Thus, the apparent anomaly of finding ytterbium on the high side of the trivalent rare earth sulfide series and on the low side of the selenide series is explained. Also explained is the fact that the T_c of YbMo_6Se_8 is lower than that of YbMo_6S_8 . In these Chevrel phases, sulfur is frequently

(15) Delk, F. S., II; Sienko, M. J. *Inorg. Chem.* **1980**, *19*, 788.

(16) Lawson, A. C.; Shelton, R. N. *Mater. Res. Bull.* **1977**, *12*, 375.

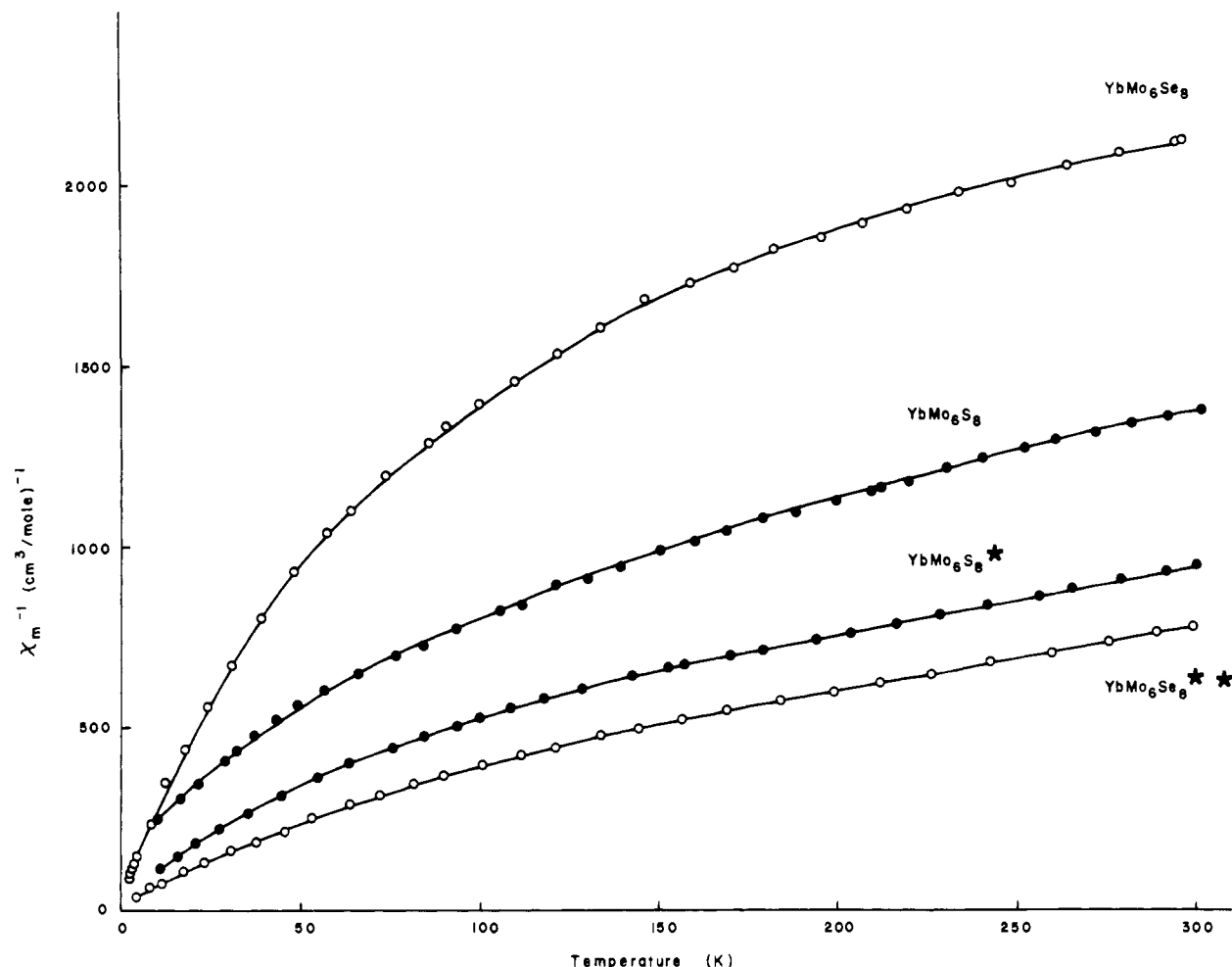
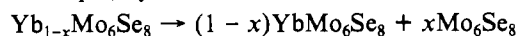


Figure 10. Reciprocal molar magnetic susceptibility vs. temperature for YbMo_6Se_8 and YbMo_6Se_8 as affected by extreme thermal treatment. The starred sample was annealed at 1520°C for 5 h; the double-starred sample was annealed at 1550°C for 16 h.

regarded to be in an oxidation state of -2 whereas selenium appears to be more like -1.7 . This means that, in going from S to Se, fewer electrons are trapped on the chalcogen, leaving more to fill up the Mo $4d E_g$ band. In Figure 3, this would correspond to moving upward from someplace near the $\text{Pb-Mo}_6\text{S}_8$ level toward the $(\text{RE})^{\text{III}}\text{Mo}_6\text{S}_8$ level. Deviating from stoichiometry, either by taking out some sulfur (electron traps) or by adding excess ytterbium (electron donors) accomplishes the same thing.

What is difficult to understand is why the T_c of YbMo_6Se_8 is so very low. Even at the minimum in the density of states, $N(E)$ is still rather large. This, of course, ignores possible effects of electron-phonon coupling, which may indeed change in going from sulfides to selenides. Another difficulty is to explain why excess ytterbium in $\text{Yb}_{1.2}\text{Mo}_6\text{Se}_8$ triggers the precipitation of Mo_6Se_8 . It would be more logical to expect appearance of Mo_6Se_8 when the system is ytterbium deficient as, for example, by the reaction



In order to confirm this fact, we extended our study of the system $\text{Yb}_{1+x}\text{Mo}_6\text{Se}_8$. Table V shows the results. When the system is deficient in ytterbium, the above reaction indeed does take place and Mo_6Se_8 appears as an impurity phase in the samples. Hence, we observe a T_c . When $0 < x < 0.1$, we observe only one phase, no impurity phase, and no T_c . For $x \geq 0.2$, as indicated in Table V, the results are strongly dependent on the heat treatment of the samples. Three samples ($x = 0.2, 0.4, 0.6$; marked *b* in the table) were prepared as usual with a slow initial rise of the temperature to 1050°C over 5 days. The resulting products on X-ray analysis showed

Table V. Crystallographic Data and Superconducting Critical Temperatures for $\text{Yb}_{1\pm x}\text{Mo}_6\text{Se}_8$

nominal compn	<i>a</i> , Å	<i>c</i> , Å	<i>c/a</i>	T_c , K	other phases
$\text{Yb}_{0.6}\text{Mo}_6\text{Se}_8$	9.481	11.890	1.2540	5.8 ($\Delta T_c = 1.15$)	Mo_6Se_8
$\text{Yb}_{0.8}\text{Mo}_6\text{Se}_8$	9.481	11.892	1.2542	5.6 ($\Delta T_c = 1.2$)	Mo_6Se_8
$\text{Yb}_{1.0}\text{Mo}_6\text{Se}_8$	9.485	11.890	1.2535		none
$\text{Yb}_{1.05}\text{Mo}_6\text{Se}_8$	9.490	11.887	1.2526		none
$\text{Yb}_{1.1}\text{Mo}_6\text{Se}_8$	9.486	11.892	1.2536		none
$\text{Yb}_{1.2}\text{Mo}_6\text{Se}_8^a$	9.485	11.892	1.2538	5.65 ($\Delta T_c = 1.2$)	Yb_2Se_3 , Mo_6Se_8
$\text{Yb}_{1.2}\text{Mo}_6\text{Se}_8^b$	9.487	11.899	1.2542		Yb_2Se_3
$\text{Yb}_{1.4}\text{Mo}_6\text{Se}_8^b$	9.484	11.892	1.2539		Yb_2Se_3
$\text{Yb}_{1.6}\text{Mo}_6\text{Se}_8^b$	9.485	11.894	1.2539		Yb_2Se_3

^a Very rapid initial heating to reach 1050°C , viz., 2 days.

^b Slow initial heating to reach 1050°C , viz., 5 days.

YbMo_6Se_8 with no change in lattice parameters and some impurity phases that were difficult to index but were neither MoSe_2 nor Mo_6Se_8 . It should be noted also that for all these samples a slight film of the green powder Yb_2Se_3 appears on the wall of the reaction tube. None of these preparations showed a superconducting T_c . In contrast, the sample ($x = 0.2$; marked *a* in the table) that had been prepared by rapid initial rise of temperature showed a T_c due to the presence of Mo_6Se_8 . Yb_2Se_3 was also observed on the wall of the reaction tube. For *b*-type materials we can write a reaction such as



where the $\text{YbMo}_6\text{Se}_{7.4}$ lies in the homogeneity range previously

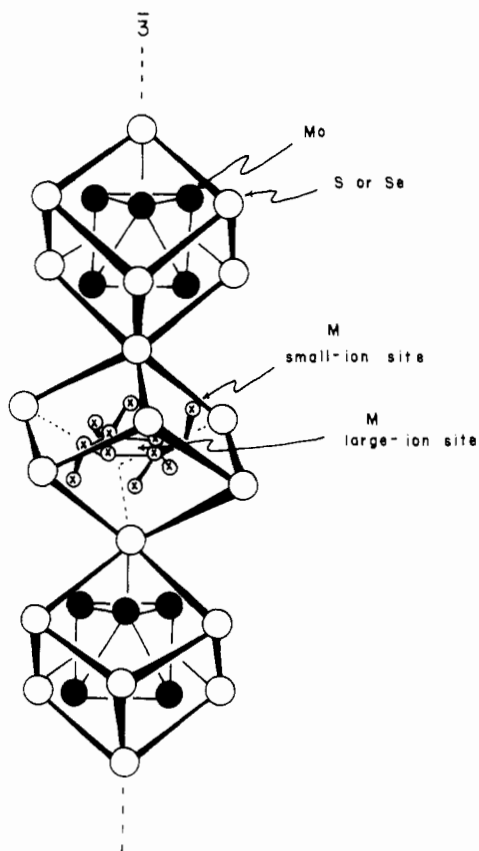
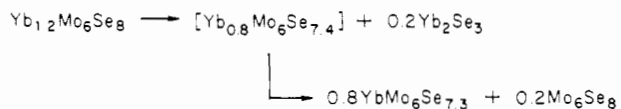


Figure 11. “Large-ion” vs. “small-ion” sites in M_xMo₆Se₈. defined in Table III. For the *a*-type material, the reaction appears to be



These findings confirm the importance of careful sample preparation. The best specimens were obtained with a slow

initial temperature increase, which allows the molybdenum and chalcogen to prereact, preventing thermal runaway and formation of another phase such as Yb₂Se₃, which is difficult to get rid of.

A final point of interest is where in these structures the ytterbium is located. In the divalent state, Yb²⁺ is large (1.02 Å) and almost certainly occupies the single “large-ion” site on the $\bar{3}$ axis between Mo₆X₈ clusters, but in the trivalent state, Yb³⁺ is considerably smaller (0.87 Å) and may partly be accommodated in one of the 12 “small-ion” sites located in a girdle around the $\bar{3}$ axis. Figure 11 shows the relative disposition of the two kinds of sites. For the large ions such as La³⁺, Pb²⁺, or Yb²⁺, there is but one site per unit cell located at the origin on the $\bar{3}$ axis. For small ions such as Fe²⁺ or Cu⁺ (or Yb³⁺?), there is a choice of 12 tetrahedral sites off the $\bar{3}$ axis. Six of the tetrahedral sites (so-called “outer sites”¹⁷) are closer to the molybdenum atoms than the other six “inner sites”. It is proposed that Yb³⁺ can be disposed either on the large-ion site or on one of the small-ion sites. If it is the latter, then it is further proposed that only Yb³⁺ that is on an “outer site”, i.e., close to Mo, can act to quench the superconductivity. For reasons that are not yet clear, it seems that selenium substituted for sulfur enhances the fraction of Yb³⁺ on the “outer” sites. EXAFS and Mössbauer studies would be extremely useful in checking out this hypothesis.

Since there are several “small-ion” sites per unit cell instead of the single “large-ion” site, it appears that excess ytterbium of materials such as Yb_{1.1}Mo₆Se₈ could be accommodated by double ytterbium occupancy (on “small-ion” sites) in some finite fraction of the unit cells.

Acknowledgment. This research was sponsored by the Air Force Office of Scientific Research under Grant No. AFOSR 80-0009 and was supported in part by the National Science Foundation and the Materials Science Center at Cornell University.

Registry No. YbMo₆S₈, 57485-88-8; YbMo₆Se₈, 59249-41-1.

(17) Yvon, K.; Paoli, A.; Flükiger, R.; Chevrel, R. *Acta Crystallogr., Sect. B* 1977, B33, 3066.